Research Square

Preprints are preliminary reports that have not undergone peer review.
They should not be considered conclusive, used to inform clinical practice,
or referenced by the media as validated information.

Automated Radiosynthesis of [^{18}F]Fluoroedaravone for Clinical Research on a Commercially Available Trasis AllinOne Radiosynthesizer

Arijit Ghosh
St Jude Children's Research Hospital
Joana Marie A. Almazan
St Jude Children's Research Hospital
Ivan E. Wang
St Jude Children's Research Hospital
Allison J. Clay
St Jude Children's Research Hospital
Spenser R. Simpson
St Jude Children's Research Hospital
Kiel D. Neumann
St Jude Children's Research Hospital
Amy L. Vavere
Amy.Vavere@STJUDE.ORG

St Jude Children's Research Hospital https://orcid.org/0009-0008-2011-8790

Research Article

Keywords: Neurodegenerative diseases, fluoroedaravone, PET, RONS, oxidative stress, Trasis AiO

Posted Date: November 4th, 2026

DOI: https://doi.org/10.21203/rs.3.rs-11368315/v1

License: This work is licensed under a Creative Commons Attribution 4.0 International License.
Read Full License

Abstract

Background

Measuring reactive oxygen and nitrogen species (RONS) in vivo remains challenging to date, thereby limiting our understanding of the role oxidative stress plays in neurodegenerative disease pathogenesis. Current PET tracers developed to detect RONS face limitations in biological stability, blood-brain barrier permeability, and RONS specificity. A novel PET tracer for RONS, [^{18}F]fluoroedaravone ([¹⁸F]FEDV), was recently reported that demonstrates high contrast in vivo with high specificity for RONS. The previously reported synthesis of [^{18}F]FEDV was performed manually, therefore, the goal of this study was to develop and optimize a robust and reproducible automated method for the synthesis of [^{18}F]FEDV on a commercially available Trasis AllinOne (AiO) radiosynthesizer for routine preclinical and clinical research use.

Results

The [¹⁸F]FEDV synthesis was adapted from a manual protocol into a fully automated two-pot, three-step process on the Trasis AiO radiosynthesizer. Optimization included varying precursor masses, radiofluorination times, temperatures, dilution conditions, purification and reformulation parameters. The optimized synthesis and purification process was completed in 105 min and produced [¹⁸F]FEDV with a radiochemical yield of 11.4% ± 1.5% (n = 50), radiochemical purity of 97.5% ± 1.4% (n = 25), chemical impurities < 100 µg/dose, and a pH of 5.0. This automated process produced [¹⁸F]FEDV with high reproducibility and reliability suitable for clinical use. The process was validated to meet USP < 823 > regulatory requirements including full QC testing on three consecutive batches.

Conclusions

An automated method for the radiochemical synthesis of [^{18}F]fluoroedaravone was developed and optimized on a commercially available Trasis AiO radiosynthesizer. This method allows for the reliable production of [^{18}F]FEDV for supporting preclinical research and first in human clinical trials.

Background

Reactive oxygen and nitrogen species (RONS) generated in mitochondria, as a by-product of the processing of molecular oxygen, play a key role in maintaining physiological balance by mediating homeostatic cellular functions in low concentrations (oxidative eustress) (Schieber et al. 2014; (Ramalingam et al. 2012). These RONS include, among others, superoxide anion ($O_2^{\cdot -}$), hydroxyl radical (OH.), hydrogen peroxide (H_2O_2), nitric oxide (NO) and molecules derived from NO (Chandimali et al. 2025; (Sarniak et al. 2016). However, when antioxidant systems are overwhelmed, excessive generation

of RONS in normal cells leads to oxidative stress and initiates a cascade of catastrophic events such as lipid peroxidation, protein and nucleic-acid oxidation, and mitochondrial permeability transition, ultimately resulting in cell death via apoptosis and necrosis (Guo et al. 2013; (Pizzino et al. 2017; (Cobb et al. 2015).

The brain is especially susceptible to such oxidative stress damage due to its high oxygen usage, an abundance of polyunsaturated lipids, iron content, and comparatively modest antioxidant reserves (Dash et al. 2025). As a result, neurodegenerative diseases such as Alzheimer's disease (AD), Parkinson's disease (PD), dementia, amyotrophic lateral sclerosis (ALS), and multiple sclerosis (MS) are linked to increased levels of oxidative stress (Rekatsina et al. 2020). Neuronal degeneration in AD patients is correlated with oxidative damage to all biomacromolecule types, as established from marked increased levels of 8-hydroxy-2-deoxyguanosine indicating DNA and RNA oxidation, as well as high levels of protein carbonyls and nitrotyrosine indicative of protein oxidation (Jiang et al. 2016; (Perry et al. 2000). Similarly, dopaminergic neurons in the brains of PD patients also exhibit hallmarks of oxidative stress, including lipid peroxidation, nucleic acid and protein oxidation, and antioxidant capacity (Jiang et al. 2016; (Bronte et al. 2025; (Wang et al. 2026). Oxidative stress is also associated with dementia as prior work has demonstrated correlations between oxidative stress biomarkers like malondialdehyde, glutathione peroxidase, protein carbonyls and cognitive decline (Altahrawi et al. 2025). Collectively, these findings indicate that uncontrolled RONS generation and oxidative stress act as a proximal driver of neuronal dysfunction and death and may be an attractive target for antioxidant and radical scavenger drug development in these diseases.

Currently, non-invasive RONS measurement in the central nervous system remains a practical barrier to studying the role oxidative stress plays in the onset and progression of neurodegenerative disease in vivo. Recent advances have included the use of magnetic resonance imaging (MRI) techniques such as hyperpolarized ^{13}C as an endogenous redox sensor for in vivo metabolic imaging (Keshari et al. 2011). Positron emission tomography (PET) is a non-invasive imaging modality with superior sensitivity and spatial resolution (Nerella et al 2022) that has been extensively used clinically to assess neuroinflammation and neurocognitive disease pathology (Vanderlinden et al. 2025; (Visser et al. 2024). To this end, several PET tracers have been developed for the non-invasive assessment of oxidative stress (Zhao et al. 2026) but with limitations. Among them are radiotracers based on the redox-sensitive scaffold of dihydroethidium, which are known to detect superoxide only via oxidative conversion to ethidium., such as [^{18}F]fluorodihydromethidine (Egami et al. 2020). Another tracer, [^{11}C]ascorbic acid has shown limited blood brain barrier permeability (Carroll et al. 2016). [^{18}F]ROStrace was designed to enhance lipophilicity and tissue retention and has been extensively studied in mouse models of oxidative stress, including AD (Hsieh et al. 2022). However, its reactivity is limited to the short-lived superoxide radical alone (Hou et al. 2018; (Wilson et al. 2017). A different category of tracers that detect oxidative stress indirectly through redox-sensitive accumulation pathways associated with hypoxia include [^{64}Cu]diacetyl-bis(N4-methylthiosemicarbazone). Although this tracer is particularly useful for assessing oxidative injury in neurodegenerative diseases such as PD where altered cellular redox states

accompany hypoxia-induced damage (Ikawa et al. 2011; (Tachibana et al. 2013), whether it specifically detects hypoxia remains uncertain (Okazawa et al. 2022).

[^{18}F]fluoroedaravone ([^{18}F]FEDV), a PET analogue of edaravone (3-methyl-1-phenyl-2-pyrazolin-5-one), which is a known free radical scavenger and an FDA-approved drug for the treatment of ALS (Witzel et al. 2022), was recently developed to study oxidative stress in vivo (Wilde et al. 2025). [^{18}F]FEDV was shown to cross the blood-brain barrier and demonstrated excellent stability in vivo. In addition, [^{18}F]FEDV was able to detect oxidative stress in several mouse models of disease including photothrombotic stroke and P301S tauopathy (Wilde et al. 2025). The broad reactivity of [^{18}F]FEDV with lipid- and water-soluble peroxyl radicals, biological stability, and blood-brain barrier penetrability warrant further research in preclinical and clinical studies.

The goal of this work was to develop a robust, reproducible, and automated method to produce [^{18}F]FEDV for routine preclinical and clinical research studies using a commercially available Trasis AllinOne radiosynthesizer yielding sufficient activity to support clinical trials with a production time of less than two hours. To this end, we optimized and validated a radiosynthesis method including quality control results from three consecutive successful syntheses in accordance with USP < 823>.

Methods

General

All chemicals were purchased from Sigma-Aldrich (St. Louis, MO), unless otherwise noted, and used without further purification. All aqueous solutions were prepared with ultrapure water (Milli-Q Integral Water Purification System, Millipore Corp.; 18.2 MΩ·cm resistivity) or sterile water for injection (USP). The radiochemical precursor 4-((tert-butoxycarbonyl)diazenyl)-N,N,N-trimethylbenzenaminium trifluoromethanesulfonate, was synthesized and characterized in-house using a previously reported method (Nebel et al. 2017). High purity anhydrous solvents, e.g., acetonitrile (99.8%) and ethanol, (> 99.5%, 200 proof, USP grade) were used without further purification.

The automated [^{18}F]FEDV synthesis method described here was developed and optimized using a commercially available Trasis AiO radiosynthesizer consisting of thirty motor units, eight gas and exhaust ports, two heating/cooling blocks and five syringe drivers that can interface with five, 6-port research cassettes custom assembled in series with tubing, syringes, reagent and reactor vials (6–20 mL capacity), and an integrated semi-preparative high performance liquid chromatography (HPLC) system. The HPLC unit is comprised of a quaternary HPLC pump, a Rheodyne valve-controlled 9 mL sample loop and injection port, and radioactivity and UV-visible detectors, all controlled by the Trasis Supervision software. The cassette assembly layout and software interface is shown in Fig. 1.

The semi-preparative HPLC unit of the Trasis AiO was cleaned with an automated program using ethanol (EtOH) and sterile water, and the final product line was cleaned and sterilized by rinsing with 10 mL

sterile water, 10 mL sterile 70% ethanol, and then dried with nitrogen prior to each synthesis run. In addition, new single-use cassettes, vials and consumables were used to avoid cross-contamination between productions.

All radioactive work was performed in a Comecer BBS2 hot cell. The radiopharmaceutical doses were measured using a Capintec CRC-15PET dose calibrator. Analytical HPLC was performed on a 1200 Series Agilent LC system using both diode array detection and a Bioscan Flow-Count radionuclide detector (Eckert & Ziegler - Bioscan). Volatile organic impurities analysis by gas chromatography (GC) was carried out using an Agilent model 8890 GC system. Both the analytical HPLC and GC equipment were controlled by Agilent's OpenLab CDS ChemStation software.

Radiosynthesis of [F]Fluoroedaravone

The automated synthesis method for [^{18}F]FEDV developed on the Trasis AllinOne module was translated from a manual method previously reported (Wilde et al. 2025). Briefly, [^{18}F]FEDV was produced by a two-pot, three-step method involving nucleophilic aromatic substitution with fluorine-18 of a 4-((tert-butoxycarbonyl)diazenyl)-N,N,N-trimethylbenzenaminium trifluoro-methanesulfonate precursor (**1** in Fig. 2).

Upon Sep Pak purification, reduction with acetic acid and zinc powder, acid hydrolysis with hydrochloric acid (10N), and condensation with ethyl acetoacetate were performed in a second reactor vial to yield the crude product. This was followed by a semi-preparative HPLC purification and reformulation of the purified [^{18}F]FEDV (**3**) in an injectable solution containing ethanolic saline.

Aqueous [^{18}F]fluoride, produced by the ^{18}O(p,n)^{18}F nuclear reaction in an IBA Cyclone® 18/9 cyclotron from ^{18}O-enriched water, was transferred from the target to a v-vial in a dose calibrator within the hot cell using helium flow (99.9999% high purity, Nexair). After measuring the activity value, the [^{18}F]fluoride solution was passed through a QMA cartridge (Myja Scientific, 46 mg) or QMA Accell Plus light cartridge (Waters, 130 mg) conditioned with 3 mL 1 M sodium bicarbonate followed by 8 mL deionized water to trap the [^{18}F]fluoride and separate it from the [^{18}O]water. The [^{18}F]fluoride was then eluted from the QMA cartridge into reactor vial 1 with a 1 mL solution of 9:1 acetonitrile-water containing 1 mg of potassium carbonate and 6 mg of Kryptofix (K222). The solvents were removed under nitrogen flow with reduced pressure and heating at 90°C for 4 minutes. A second azeotropic evaporation was performed by addition of 1 mL of acetonitrile followed by solvent removal under nitrogen flow with reduced pressure and heating at 90°C for 6 minutes. This was followed by the addition of 3.0 ± 0.5 mg of 4-((tert-butoxycarbonyl)diazenyl)-N,N,N-trimethylbenzenaminium trifluoromethanesulfonate precursor (**1**) dissolved in 0.4 mL acetonitrile to the dried [^{18}F]KF in the reactor vial, which was then sealed and heated at various temperatures (85 ºC, 95°C, 105°C) for 1 or 7 minutes. Post fluorination, the reactor vial was cooled (50°C or 20°C) and held for different times (up to 10 minutes) and the intermediate (**2**) was diluted in aqueous solution (water, aqueous sodium carbonate pH 9.3 ± 0.2, or 0.5% (w/v) sodium

ascorbate) followed by a second wash. The reactor vial contents were then passed through a tC18 Plus Light Sep Pak cartridge (Waters, 145 mg, conditioned with 5 mL ethanol followed by 10 mL Milli-Q water). The cartridge was washed with 3 mL water to remove any polar impurities, followed by nitrogen gas to purge it. Next, the trapped ^{18}F-fluorinated intermediate (**2**) was eluted from the cartridge with 1 mL glacial acetic acid into a reactor vial 2 that was preloaded with 25 ± 5 mg zinc dust. The vial was sealed and heated to 85°C for 1 minute with a slow nitrogen flow to simulate stirring. The vial was then cooled to 50°C and a mixture of 250 µL of ethyl acetoacetate and 250 µL of 10N hydrochloric acid (HCl) was added. The vial was left to vent for 1 minute until the evolution of hydrogen gas ceased, then sealed and heated at 85°C or 95°C for 20 minutes followed by cooling to 50°C. A 2.5 mL solution of Milli-Q water containing 125 mg sodium acetate was then added to the vial, and the solution was filtered through a 13 mm, 0.45 µm PVDF syringe filter and injected onto a Synergi Hydro-RP C18 column (Phenomenex, 10 µm, 250 × 10 mm, 80 Å) under an isocratic flow of 65:35 acetate buffer (0.2 M acetic acid/0.05 M sodium acetate, pH 4.1)/EtOH at 3.5 mL/min with UV-visible (254 nm) and radioactive detection for purification by semi-preparative reversed-phase (RP) HPLC. In addition, purification of the crude product was attempted with a modified acetate buffer of pH 5.1 and varied ethanol percentages to test if reformulation could be eliminated by reducing the percent ethanol in the final product. Three conditions were tested 1) 35% EtOH for 10 min at 3.5 mL/min, then switched to 5% EtOH at the same flow rate 2) 35% EtOH for 5 min at 3.5 mL/min, then switched to 5% EtOH at the same flow rate 3) 35% EtOH for 5 min at 3.5 mL/min, then switched to 5% EtOH at 5 mL/min.

If reformulation was needed, the purified fraction was collected into a 100 mL vial containing 40, 80, or 150 mL of water or acetate buffer (0.2 M acetic acid/0.05 M sodium acetate) for dilution. The diluted fraction was then transferred through one of three HLB cartridges with 10 mg, 30 mg, or 140 mg substrate (Waters, conditioned with 5 mL ethanol followed by 10 mL Milli-Q water), and subsequently washed with 10 mL Milli-Q water. The pure product was then eluted from the cartridge with 0.5, 1.0, or 1.2 mL ethanol directly into a vial containing 10 mL saline. The reformulated [^{18}F]FEDV (**3**) was finally pushed through a sterilizing filter (Millipore, Cathivex-GV, 0.22 µm) into a sterile final product vial assembly.

The automated method included rinsing of the manifold assembly along with all tubing with water and dried with nitrogen gas at every step in between addition of reagents to avoid cross-contamination. Several steps such as addition of reagents, trapping on cartridges, and subsequent elutions into reactor vials were followed by multiple nitrogen gas pushes for minimal loss of products due to adherence to the manifold and tubing. Steps involving transfer of reaction solutions from reactor vials were followed with an additional wash step to minimize residual product remaining behind in the vials.

Quality Control Testing & Validation

An analytical RP-HPLC method was used to characterize the [^{18}F]FEDV intermediate (**2**) formed immediately after radiofluorination of the Boc-protected diazo-trimethylammonium triflate precursor (**1**)

for optimization. Analysis was performed on a Synergi Hydro-RP C18 analytical column (250 × 4.6 mm, 4 µm) with an isocratic mobile phase of a 30:70 (v/v) mixture of water and acetonitrile at a flow rate of 1 mL/min, and UV (254 nm) and radioactive detection. The radiochemical purity (RCP) of radiofluorinated intermediate (**2**), expressed as a percentage, was determined from the peak area of the intermediate and the total peak areas in the chromatogram as detected by the radioactivity detector.

Several quality control tests were performed on the [^{18}F]FEDV product (**3**) to assure the quality of the final dose in accordance with guidelines from USP < 823 > Radiopharmaceuticals for Positron Emission Tomography-Compounding. The final product was confirmed to be clear and colorless with no visual evidence of cloudiness or particulate matter per USP < 631 > Color and Achromicity.

[^{18}F]FEDV (**3)** was injected onto a Synergi Hydro-RP C18 analytical column (Phenomenex, 250 × 4.6 mm, 4 µm) for HPLC analysis. An isocratic mobile phase containing a 50:50 (v/v) mixture of acetate buffer (0.2 M acetic acid/0.05 M sodium acetate, pH 4.1) and acetonitrile with a flow rate of 1.25 mL/min was used to analyze identity and purity of the product with UV (254 nm) and radioactive detection. A non-radioactive [^{19}F]FEDV solution (0.1 mg/mL in HPLC eluent mixture) was used as a standard for radiochemical identity of [^{18}F]FEDV via retention time comparison (retention times within 15% of each other). The RCP of [^{18}F]FEDV, expressed as a percent, was determined from the peak area of [^{18}F]FEDV and the total peak areas in the chromatogram as detected by the radioactivity detector. The product was analyzed in duplicate, in addition to a 1:1 (v/v) co-injection with the reference standard.

To determine the quantity of volatile organic impurities/residual solvents in the final sample, an aliquot of [^{18}F]FEDV (**3**, 0.5 µL) was analyzed by gas chromatography using a DB-WAX column (J & W 122–7032, 30 m x 250 µm x 0.25 µm). The oven temperature was set to 60°C for 1 minute, then ramped to 140°C at a rate of 40°C/min and held for 1 minute. The total run time was 4 minutes, and the front inlet heater was set to 250°C. The split ratio was 15:1, hydrogen flow was 40 mL/min, and the air flow was 400 mL/min. The GC peak retention times (RT) and areas were compared to standards of ethyl acetate (0.01%; RT ~ 1.29 min), ethanol (1.0%; RT ~ 1.38 min), and acetonitrile (0.01%; RT ~ 1.59 min). The amount of each component was calculated based on the ratio of peak areas for the samples vs. the standard.

Residual Kryptofix® (K222) was determined by color spot test on silica based on the method by Mock et al. (Mock et al. 1997). The FDA has proposed a maximum permissible level of 50 µg/mL of Kryptofix® 222 in 2-[^{18}F]FDG, therefore we proposed this maximum permissible level is appropriate for the [^{18}F]FEDV final product (**3**). A strip of plastic-backed silica TLC plate was prepared by soaking in an acidic iodoplatinate solution and dried. Aliquots of 2 µL each of final product, water, and 50 µg/mL K222 standard were spotted on the iodoplatinated test strip. Kryptofix® 222 in the standard will stain the center of the spot a dark color with a blue ring while the water standard will remain light in the center. The product was compared to the standard to confirm that the color change is lighter than the standard limit of 50 µg/mL. In addition, the pH of the final formulation of [^{18}F]FEDV (**3**) was tested by spotting on a narrow range pH indicator strip and comparing it with the color range chart provided by the

manufacturer. The final drug product was tested for the presence of bacterial endotoxins utilizing the Endosafe®-PTS™ unit (Charles River) to determine the endotoxin concentration in a sample in accordance to USP < 85 > Bacterial Endotoxins Test. Sterility was tested using the direct inoculation method into trypticase soy broth and fluid thioglycolate media as recommended by the USP < 71 > Sterility Tests, and the samples were observed over 14 days.

The radionuclidic identity of the final product (**3**) was determined by observing the radioactive half-life ($t_{½}$) using a Capintec CRC-15PET dose calibrator with two measurements separated by an interval of 10 minutes. Radionuclidic purity was determined using a Canberra MCA System. Testing took place at least 8 days after production with an acquisition time of 12 hours, ensuring adequate spectral resolution for impurity identification. This approach follows standard industry practices, including USP < 821 > Radioactivity, which requires sufficient decay time to detect potential long-lived impurities. The assessment was performed by the Cyclotron Facility at the Mallinckrodt Institute of Radiology, Washington University in St. Louis, using gamma spectrometry to compare the emission spectrum against known radionuclide decay schemes and calibration standards. Filter integrity test using bubble point was also performed on the sterile filter with the manufacturer's specified point of > 50 psi after passing 10 mL of sterile water due to the higher ethanolic content of the final product.

Results

Radiosynthesis of [^{18}F]Fluoroedaravone

The goal of this study was to automate and optimize the synthesis of [^{18}F]fluoroedaravone on a Trasis AllinOne radiosynthesizer facilitating easy access to the tracer for preclinical and clinical studies. We based our synthesis script on the previously published manual method with some modifications and optimizations (Wilde et al. 2025).

The efficiency of the radiofluorination step was tested in acetonitrile using 3.0 ± 0.5 mg of precursor (**1**) at varied times (1, 7 min) and temperatures (85°C, 95°C,105°C) on the Trasis AiO and the radiochemical conversion (RCC) was compared with the manual synthesis results (see Table 1).

Table 1

^{18}F-Intermediate optimization results.

Temperature (°C)	Time (min)	Manual RCC (%)	Trasis RCC (%)
85	1	97.9	97.6 ± 0.3 (*n* = 3)
85	7	88.1	39.0 (*n* = 2)
95	7	---	32.1 (*n* = 2)
105	7	---	12.0 (*n* = 2)

The highest RCC to the radiofluorinated intermediate (**2**) of 97.6% ± 0.3% was obtained by reacting 3.0 ± 0.5 mg of precursor (1) dissolved in 0.4 mL of acetonitrile with azeotropically distilled fluorine-18 at 85°C for 1 minute. Increasing the precursor mass up to 4.5 mg did not affect the RCC of the intermediate significantly at all (~ 69–70%, *n* = 2). The fluorinated intermediate demonstrated stability in acetonitrile for up to 90 minutes, consistent with results from the manual method. Reactions conducted at higher temperatures or for longer durations resulted in decreased RCC, falling to 32.1% at 95°C and 12.0% at 105°C.

Additionally, the stability of the intermediate (**2**) upon addition of various aqueous solutions as diluent (an essential step before tC18 purification) was assessed with cooling to different temperatures and holding for various durations, as listed in Table 2.

Table 2

^{18}F-Intermediate Preparation for tC18 purification post 1 min reaction at 85°C.

Reactor Cooling	Reagent added	Manual RCC(%)	Trasis RCC(%)
50°C + 0 min hold	Water	94.7	52.8 (*n* = 2)
20°C + 10 min hold	Water	---	64.1 (*n* = 2)
20°C + 10 min hold	0.5% (w/v) sodium ascorbate	---	0
20°C + 10 min hold	Aq. sodium carbonate (pH 9.3 ± 0.2)	---	70.1 ± 0.35 (*n* = 3)

Next, the semi-preparative HPLC conditions were optimized to explore the possibility of retrieving the pure product in < 10% ethanol (v/v) directly without the need for reformulation, which would reduce the total synthesis run time and ultimately increase activity yields. The HPLC conditions tested and their outcomes are listed in Table 3.

Table 3

[^{18}F]FEDV semi-preparative HPLC conditions optimization results.

Run	%EtOH-1	Flow-1 (mL/min)	Time switch (min)	%EtOH-2	Flow-2 (mL/min)	[^{18}F]FEDV RT (min)	Peak width (min)	%EtOH in product (GC)
1	35	3.5	10	5	3.5	17	2.5	**30.1**
2	35	3.5	5	5	3.5	**40**	**30**	6.6
3	35	3.5	5	5	5	**20**	**20**	5.3

The total synthesis time for [^{18}F]FEDV (**3**) was approximately 105 minutes including the second set of reactions at 85°C for 20 minutes, semi-preparative HPLC purification of the crude product, and reformulation. Under these conditions, [^{18}F]FEDV was produced with a radiochemical yield (RCY) of

11.4% ± 1.5% (*n* = 50) and an end of synthesis (EOS), average, non-decay corrected radiochemical yield of 5.9% ± 0.8% (*n* = 50), comparing very well with the manual method (Wilde et al. 2022). The current reported method has the benefit of being robust, fully automated and utilizing single-use, cassettes. Figure 3 shows a schematic representation of the steps in our finalized radiosynthesis, purification and reformulation of [^{18}F]FEDV (**3**) on the Trasis AiO.

Quality Control Testing & Validation

[^{18}F]FEDV (**3**) was routinely synthesized with 97.5% ± 1.4% (*n* = 25) RCP, an HPLC retention time (RT) of 4.1 minutes, and without any discernable chemical impurities. Figure 4 shows HPLC chromatograms of the [^{18}F]FEDV final product and a 1:1 (v/v) co-injection with the non-radioactive FEDV standard, thereby establishing its radiochemical identity. Gas chromatography analysis of [^{18}F]FEDV showed an obvious presence of ethanol, being an excipient in the final formulation (**Supplementary Information** Fig. 1).

Three process validation syntheses were conducted to qualify the radiosynthesis for clinical research production and IND submission, and these results are shown in Table 4.

Table 4

[^{18}F]Fluoroedaravone final dose process validation results.

Test	Specification	Batch 1	Batch 2	Batch 3
Total activity @ EOS	N/A	**2157 MBq (58.3 mCi)**	**2694 MBq (72.8 mCi)**	**2901 MBq (78.4 mCi)**
Concentration @ EOS	N/A	**193 MBq/mL (5.2 mCi/mL)**	**250 MBq/mL (6.7 mCi/mL)**	**259 MBq/mL 7 mCi/mL**
Visual Appearance	Clear, colorless, and free of particulates	**Pass**	**Pass**	**Pass**
pH	4.5–7.5	**5.0**	**5.0**	**5.0**
Radiochemical Identity & Purity	≥ 90% [^{18}F]FEDV RT within 15% of std.	RCP: **97.29%** RT Std: **3.900 min** RT Rad: **4.092 min** Difference: **4.92%**	RCP: **98.08%** RT Std: **3.891 min** RT Rad: **4.083 min** Difference: **4.93%**	RCP: **97.30%** RT Std: **3.877 min** RT Rad: **4.067 min** Difference: **4.9%**
Chemical Impurities	[$^{18/19}$F]FEDV ≤ 5 µg /mL ≤ 100 µg impurities /dose	[$^{18/19}$F]FEDV conc.: **< 2.39 µg/mL** Impurities: **≤ 50 µg /dose**	[$^{18/19}$F]FEDV conc.: **< 2.15 µg/mL** Impurities: **≤ 50 µg /dose**	[$^{18/19}$F]FEDV conc.: **< 1.95 µg/mL** Impurities: **≤ 50 µg /dose**
Radionuclidic Identity	Observed $t_{½}$ is 105 to 115 minutes	**111.32 min**	**111.26 min**	**106.3 min**
Volatile Organic Impurities and Ethanol content	Ethyl Acetate ≤ 0.5%	**< 0.001%**	**< 0.001%**	**< 0.001%**
	Ethanol ≤ 10%	**9.936%**	**9.038%**	**8.415%**
	Acetonitrile ≤ 0.041%	**< 0.001%**	**< 0.001%**	**< 0.001%**
Bacterial Endotoxin (LAL)	≤ 175 EU/dose	**< 2.50 EU/mL**	**< 2.50 EU/mL**	**< 2.50 EU/mL**
Filter Integrity	≥ 50 psi breaking pressure	**56.4 psi**	**55.0 psi**	**56.8 psi**
Sterility	no growth observed over 14 days	**Pass**	**Pass**	**Pass**

Test	Specification	Batch 1	Batch 2	Batch 3
Radionuclidic Purity	≥ 99.5% ^{18}F	**100%**	**100%**	**100%**

In addition, the [^{18}F]FEDV final product (**3**) was found to be stable over four hours in the final dose formulation, with the radiochemical purity falling below 90% after the four-hour (240 min) window, as indicated by the dotted lines in Fig. 5 below.

Discussion

The optimization and automation of the synthesis of [^{18}F]fluoroedaravone was achieved to support routine clinical research production on a Trasis AllinOne radiosynthesizer. We were successful in completing validation syntheses to support an IND application for use of this tracer in clinical research.

We previously tested and found (results not included) that a second azeotropic evaporation step after the initial fluorine-18 elution on the Trasis AiO resulted in a 25% increase in fluorine incorporation (Vavere et al. 2025). A third azeotropic step, however, did not improve labeling efficiency any further. As a result, we opted for two azeotropic drying steps. Furthermore, we tested two anion exchange cartridges; QMA Accell Plus light vs. QMA Myja Scientific for their fluoride trapping and release efficiencies on the Trasis AiO but did not find any significant difference between the two.

The ^{18}F-intermediate (**2**) was found to degrade upon the addition of water, with the extent of degradation being more severe on the Trasis AiO (~ 53%, *n* = 2) compared to the manual method (~ 94%, *n* = 2). In both cases, the degradation increased over time. To rule out radiolysis as the cause of degradation, the water was replaced with a 0.5% (w/v) solution of sodium ascorbate as a radioprotectant. However, this substitution resulted in the complete disappearance of the intermediate peak. As the compound remained stable on the column during HPLC analysis, it was hypothesized that the extent of cooling after the radiofluorination reaction may be the cause of degradation. As azocarboxylates are known to possess thermal instability (Hirose et al. 2016), we found that cooling to 20°C and holding for 10 minutes resulted in an improved RCC of ~ 64% (*n* = 2), not improving at longer times. Substituting the water with an aqueous sodium carbonate solution (pH 9.3 ± 0.2) led to further improvement resulting in a RCC of 70.1% ± 0.35% (n = 3). This is possibly due to stabilization of the Boc-protected diazo intermediate under basic conditions and elevated temperature. Based on these results, we decided to cool the intermediate to 20°C for at least 10 minutes followed by dilution with sodium carbonate solution (pH 9.3 ± 0.2). Increasing the precursor mass beyond 3 mg up to 4.5 mg did not have any significant effect on the intermediate yield. Representative HPLC chromatograms for the analysis of the ^{18}F-fluorinated intermediate are shown in **Supplemental Information** Fig. 2.

Next, we tested the tC18 cartridge loading and intermediate (**2**) recovery percentages on the Trasis AiO. Initially, we found that ~ 70% (*n* = 2) of the intermediate was being transferred to the cartridge due to residual losses from adherence to the reactor vial (after accounting for the impurities that are not

retained on the cartridge). However, adding a second wash step with 3 mL of the sodium carbonate solution (pH 9.3 ± 0.2) increased the trapping to > 85% consistently (*n* = 3). Recovery of the trapped intermediate was found to be > 92% (*n* = 2), with 1 mL glacial acetic acid.

Another distinctive modification that was incorporated in the automated method compared to the manual synthesis was combining the ethyl acetoacetate and concentrated HCl in one reagent vial, since the original method called for adding 100 µL of each separately, which is practically impossible on the Trasis due to the relatively large dead volumes in the tubing and manifold. We found that starting with a mixture of 250 µL each yielded the required final volume of ~ 200 µL due to physical losses from adherence to the manifold and tubing. Combining the reagents, however, did not affect synthesis chemistry and helped reduce the overall synthesis time. In addition, increasing the second reaction temperature to 95 ºC did not affect the RCY of the final product at all.

The semi-preparative RP-HPLC method (less than 17 min run time) used for purification of the crude product resulted in good separation of unreacted ^{18}F-labeled impurities (RT ~ 7-11.5 min), unreacted precursor (RT ~ 9 min) from the [^{18}F]FEDV product (**3**; RT ~ 14 min, **Supplemental Information** Fig. 3). The retention time of [^{18}F]FEDV was established by comparison with the non-radioactive FEDV standard under the same conditions. While testing the alternate HPLC conditions to directly collect the final product in < 10% without needing reformulation, it was imperative to start with a higher percentage of ethanol (35%) to remove all non-polar impurities including any unreacted precursor, as well as shorten the [^{18}F]FEDV retention time. GC results revealed that the time taken to completely switch from 35% to 5% ethanol in the column was ~ 20 minutes. With these findings in mind, three conditions involving an acetate buffer of pH 5.1 and various ethanol percentages were tested in an attempt to reduce the amount of ethanol while keeping the time of purification reasonable. As shown in Table 3 in the results section above, under condition 1, the [^{18}F]FEDV product eluted at ~ 17 minutes, however the EtOH content in the dose was still 30.1%. Conditions 2 and 3 led to significantly broader product peaks (> 25 min) with late retention times in both cases, although < 10% ethanol was achieved in the products. Hence, we decided to move forward with the original isocratic method of 35% ethanol and the acetate buffer.

Next, a few reformulation parameters were tested including the dilution buffer. Although the manual method used water to dilute the collected HPLC fraction of pure [^{18}F]FEDV (**3**), substituting with 80 mL of 0.2 M acetic acid/0.05 M sodium acetate buffer (pH 4.1) led to an increase in RCY by ~ 2% (*n* = 2). This is possibly due to stabilization of the ketone form of fluoroedaravone under slightly acidic conditions. The 80 mL volume led to a ~ 30-fold dilution of the ethanol in the collected product fraction resulting in optimal trapping on the HLB light cartridge. Increasing the volume beyond 80 mL did not make any significant difference but increased the HLB loading time by several minutes. In addition, we found the HLB light cartridge (30 mg) provided the most effective recovery of pure [^{18}F]FEDV (90% loading, 80% recovery), compared to the HLB Oasis plus 140 mg (95% loading, 41% recovery) and HLB 10 mg (56% loading, 82% recovery) cartridges, when eluted with 1 mL ethanol manually. However, percent recovery

from the HLB light cartridge on the Trasis was slightly lower using 1.0 mL ethanol (~ 60%, *n* = 2) compared to when done manually due to partial loss of ethanol in the manifold and tubing. Increasing the ethanol volume to 1.2 mL resulted in an improvement to 76.2 ± 0.5% (*n* = 3) recovery of the final product. Going beyond 1.2 mL, however, did not improve the recovery any further.

Chemical and radiochemical purity were determined by analytical RP-HPLC using an optimized method that reduced the overall duration of analysis. By adjusting from an isocratic 65:35 acetate buffer (0.2 M acetic acid/0.05 M sodium acetate, pH 4.1)/ethanol system to an isocratic 50:50 acetate buffer/acetonitrile system, lower pressures were observed and therefore higher flow rates (1 mL/min to 1.25 mL/min) could be used. With the new conditions, the [^{18}F]FEDV product (**3**) eluted at 4.1 min (vs. ~ 9 min in the previous method) and by increasing the organic concentration, additional trace non-polar impurities could also be identified (~ 10 min). The optimization resulted in a 12-minute method which significantly decreased the overall analysis time from the previous 20-minute method. Using this new method, we observed [^{18}F]FEDV RCP > 97% with no detectable chemical impurities.

Due to the absence of an integrable [^{19}F]FEDV UV peak in the [^{18}F]FEDV samples, molar activity was calculated using the instrument limit of integration which was determined to be 10 ng. This resulted in a calculated molar activity of > 400 Ci/mmol. Due to a very low cold mass, we opted not to calculate molar activity for all further productions. Additionally, the FDA defines microdosing as masses of < 100 µg therefore, if the entire 11.2 mL dose were to be injected this would result in a maximum of 22.4 µg which further reinforced our decision not to include molar activity as a quality control criterion.

Conclusions

In summary, an automated method for the radiochemical synthesis of [^{18}F]fluoroedaravone was developed and optimized on a commercially available Trasis AllinOne radiosynthesizer. This method allows reliable production of [^{18}F]fluoroedaravone with 11.4% ± 1.5% (*n* = 50) radiochemical yield, high radiochemical purity (> 97%), no discernable chemical or volatile organic impurities, suitable for human use. Finally, the synthesis was process-validated with comprehensive quality control testing in accordance with USP < 823>, qualifying it for clinical research applications.

Abbreviations

AD Alzheimer’s disease

AiO AllinOne

ALS Amyotrophic lateral sclerosis

DNA Deoxyribonucleic acid

EOS End of synthesis

EtOH Ethanol

FDA Food and Drug Administration

FDG Fluorodeoxyglucose

FPV Final product vial

FEDV Fluoroedaravone

GC Gas chromatography

H_2O Water

HCl Hydrochloric acid

RP-HPLC Reversed phase high performance liquid chromatography

IND Investigational new drug

K222 Kryptofix® 2.2.2

K_2CO_3 Potassium carbonate

KF Potassium fluoride

MCA Multi channel analyzer

MeCN Acetonitrile

MRI Magnetic resonance imaging

MS Multiple sclerosis

PD Parkinson’s disease

PET Positron emission tomography

PTS Portable test system

PVDF Polyvinylidene fluoride

RCC Radiochemical conversion

RCP Radiochemical purity

RCY Radiochemical yield

RNA Ribonucleic acid

RONS Reactive oxygen and nitrogen species

RT Retention time

TLC Thin layer chromatography

USP United States Pharmacopeia

UV Ultra-violet

Declarations

Acknowledgements

The authors would like to thank the staff of the Molecular Imaging Core at St. Jude Children's Research Hospital. They would also like to thank Thomas Voller of the Cyclotron Facility at the Mallinckrodt Institute of Radiology, Washington University, St. Louis for his help with analyzing the radionuclidic purity of the validation samples.

Authors' Contributions

AG, AJC, IEW, SS, ALV and KDN designed the studies. AG, AJC, IEW, and JAA carried out the experiments, AG and IEW prepared the manuscript. All authors read, edited and approved the final manuscript.

Funding

This study was funded by NIH R01EB028338 (KDN), R01AG093113 (KDN), and R01AI192221 (KDN) and the American Lebanese Syrian Associated Charities (ALSAC).

Data Availability

The data used and/or analyzed during the current study are available from the corresponding author on reasonable request.

Ethics approval and consent to participate

Not applicable.

Consent for publication

Not applicable.

Competing interests

The authors declare that they have no conflict of interest with regard to this study.

References

1. Altahrawi AY, James AW, Shah ZA. The role of oxidative stress and inflammation in the pathogenesis and treatment of vascular dementia. Cells. 2025;14(8):609.
2. Bronte A, Prieto E, Quincoces G, Erro E, Arbizu J. The basics of PET molecular imaging in neurodegenerative disorders with dementia and/or parkinsonism. Eur Radiol. 2025;35(8):4621–34.
3. Carroll VN, Truillet C, Shen B et al. [^{11}C]Ascorbic acid [^{11}C]dehydroascorbic acid, an endogenous redox pair for sensing reactive oxygen species using positron emission tomography. 2016;52(27):4888–90.
4. Chandimali N, Bak SG, Park EH, et al. Free radicals and their impact on health and antioxidant defenses: A review. Cell Death Discov. 2025;11(1):19.
5. Cobb CA, Cole MP. Oxidative and nitrative stress in neurodegeneration. Neurobiol Dis. 2015;84:4–21.
6. Dash UC, Bhol NK, Swain SK, et al. Oxidative stress and inflammation in the pathogenesis of neurological disorders: mechanisms and implications. Acta Pharm Sin B. 2025;15(1):15–34.
7. Egami H, Nakagawa S, Katsura Y, et al. F-labeled dihydromethidine: positron emission tomography radiotracer for imaging of reactive oxygen species in intact brain. Org Biomol Chem. 2020;18(12):2387–91.
8. Guo C, Sun L, Chen X, Zhang D. Oxidative stress, mitochondrial damage and neurodegenerative diseases. Neural Regen Res. 2013;8(21):2003–14.
9. Hirose D, Gazvoda M, Kosmrlj J, Taniguchi T. Advances and mechanistic insight on the catalytic Mitsunobu reaction using recyclable azo reagents. Chem Sci. 2016;7(8):5148–59.
10. Hou C, Hsieh CJ, Li S, et al. Development of a positron emission tomography radiotracer for imaging elevated levels of superoxide in neuroinflammation. ACS Chem Neurosci. 2018;9(3):578–86.
11. Hsieh CJ, Hou C, Zhu Y, et al. [^{18}F]ROStrace detects oxidative stress in vivo and predicts progression of Alzheimer's disease pathology in APP/PS1 mice. EJNMMI Res. 2022;12(1):43.
12. Ikawa M, Okazawa H, Kudo T, Kuriyama M, Fujibayashi Y, Yoneda M. Evaluation of striatal oxidative stress in patients with Parkinson's disease using [^{62}Cu]ATSM PET. Nucl Med Biol. 2011;38(7):945–51.
13. Jiang T, Sun Q, Chen S. Oxidative stress: A major pathogenesis and potential therapeutic target of antioxidative agents in Parkinson’s disease and Alzheimer’s disease. Prog neurobiol. 2016;147:1–19.
14. Keshari KR, Kurhanewicz J, Bok R, Larson PEZ, Vigneron DB, Wilson DM. Hyperpolarized ^{13}C dehydroascorbate as an endogenous redox sensor for in vivo metabolic imaging. Proc. Natl Acad. Sci. 2011;108:18606-11.
15. Mock BH, Winkle W, Vavrek MT. A color spot test for the detection of Kryptofix 2.2.2 in [^{18}F]FDG preparations. Nucl Med Biol. 1997;24(2):193–5.

16. Nebel N, Strauch B, Maschauer S, et al. [¹⁸F]Fluorophenylazocarboxylates: design and synthesis of potential radioligands for dopamine D3 and mu-opioid receptor. ACS Omega. 2017;2(12):8649–59.
17. Nerella SG, Singh P, Sanam T, Digwal CS. PET molecular imaging in drug development: the imaging and chemistry perspective. Front Med (Lausanne). 2022;9:812270.
18. Okazawa H, Ikawa M, Tsujikawa T, et al. Cerebral oxidative stress in early Alzheimer's disease evaluated by 64Cu-ATSM PET/MRI: A preliminary study. Antioxidants. 2022;11(5):1022.
19. Perry G, Nunomura A, Hirai K, Takeda A, Aliev G, Smith MA. Oxidative damage in Alzheimer's disease: the metabolic dimension. Int J Dev Neurosci. 2000;18(4–5):417–21.
20. Pizzino G, Irrera N, Cucinotta M, et al. Oxidative stress: Harms and benefits for human health. Oxid Med Cell Longev. 2017. 10.1155/2017/8416763.
21. Ramalingam M, Kim SJ. Reactive oxygen/nitrogen species and their functional correlations in neurodegenerative diseases. J Neural Transm (Vienna). 2012;119(8):891–910.
22. Rekatsina M, Paladini A, Piroli A, Zis P, Pergolizzi JV, Varrassi G. Pathophysiology and therapeutic perspectives of oxidative stress and neurodegenerative diseases: A narrative review. Adv Ther. 2020;37(1):113–39.
23. Sarniak A, Lipinska J, Tytman K, Lipinska S. Endogenous mechanisms of reactive oxygen species (ROS) generation. Postepy Hig Med Dosw (Online). 2016;70:1150–65.
24. Schieber M, Chandel NS. ROS function in redox signaling and oxidative stress. Curr Biol. 2014;24(10):R453–62.
25. Tachibana I, Nishimura Y, Shibata T, et al. A prospective clinical trial of tumor hypoxia imaging with 18F-fluoromisonidazole positron emission tomography and computed tomography (F-MISO PET/CT) before and during radiation therapy. J Radiat Res. 2013;54(6):1078–84.
26. Vanderlinden G, Vandenberghe R, Vandenbulcke M, Laere KV. The current role of tau PET imaging in neurodegeneration. Semin Nucl Med. 2025;55(4):548–64.
27. Vavere AL, Clay AJ, Ghosh A, Almazan JM, Brown MJ, Simpson S, Neumann KD. Automated radiosynthesis of [^{18}F]fluoromannitol for clinical research on a commercially available trasis allinone radiosynthesizer. EJNMMI Radiopharm Chem. 2025;10:69.
28. Visser M, O'Brien JT, Mak E. In vivo imaging of synaptic density in neurodegenerative disorders with positron emission tomography: A systemic review. Ageing Res Rev. 2024. 10.1016/j.arr.2024.102197.
29. Wang QQ, Zhang HD, Liu PY, et al. Perillaldehyde reduces mitochondrial oxidative stress damage by regulating KCNT2/NR1D1 protein activity in vascular dementia rats. Mol Biol Rep. 2026;53(1):117.
30. Wilde JH, Sun YY, Simpson SR, et al. A positron emission tomography tracer for the imaging of oxidative stress in the central nervous system. Nat Biomed Eng. 2025;9(6):716–29.
31. Wilson AA, Sadovski O, Nobrega JN, et al. Evaluation of a novel radiotracer for positron emission tomography imaging of reactive oxygen species in the central nervous system. Nucl Med Biol. 2017;53:14–20.

32. Witzel S, Maier A, Steinbach R, et al. Safety and effectiveness of long-term intravenous administration of edaravone for treatment of patients with amyotrophic lateral sclerosis. JAMA Neurol. 2022;79(2):121–30.
33. Zhao T, Patel JS, Ran C, Liang SH. Advances in PET imaging of oxidative stress: tracer innovation, mechanistic insight, and translational potential. Eur J Nucl Med Mol Imaging. 2026;53(5):1373–9.

Figures

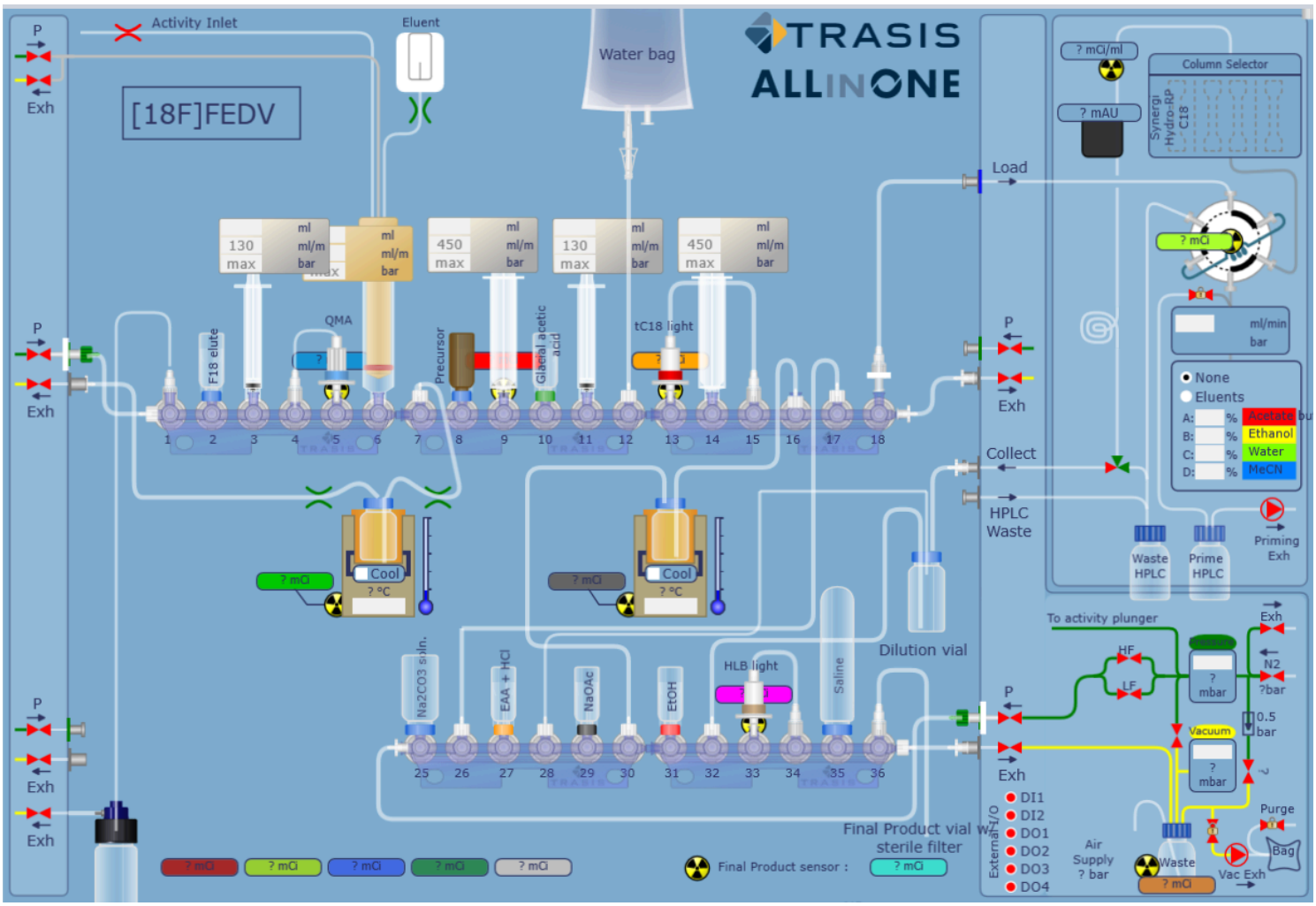


Figure 1

Cassette assembly layout for Trasis AllinOne synthesis of [^{18}F]Fluoroedaravone.

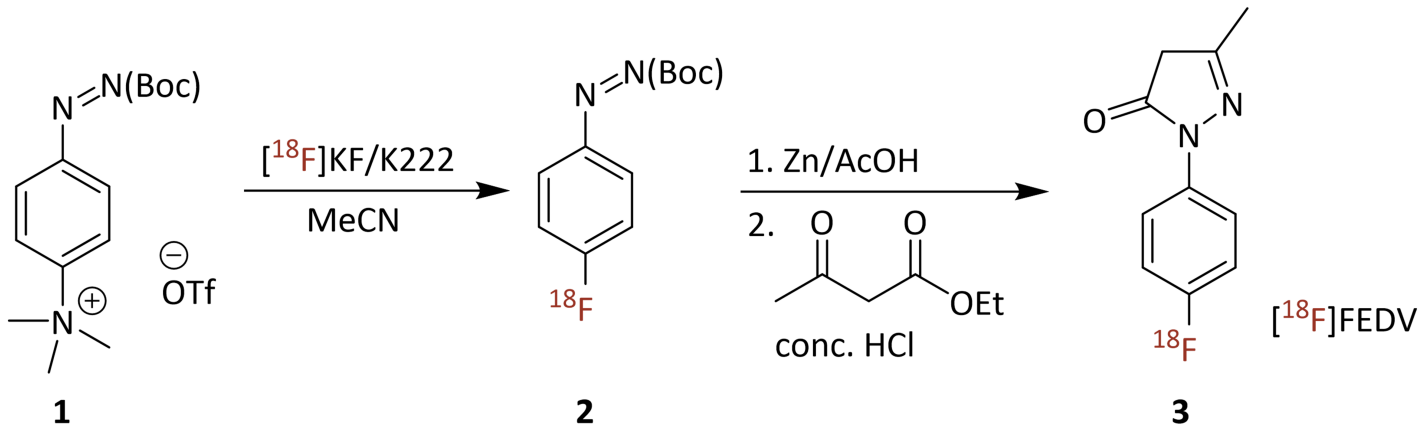


Figure 2

Radiosynthesis scheme of [^{18}F]Fluoroedaravone.

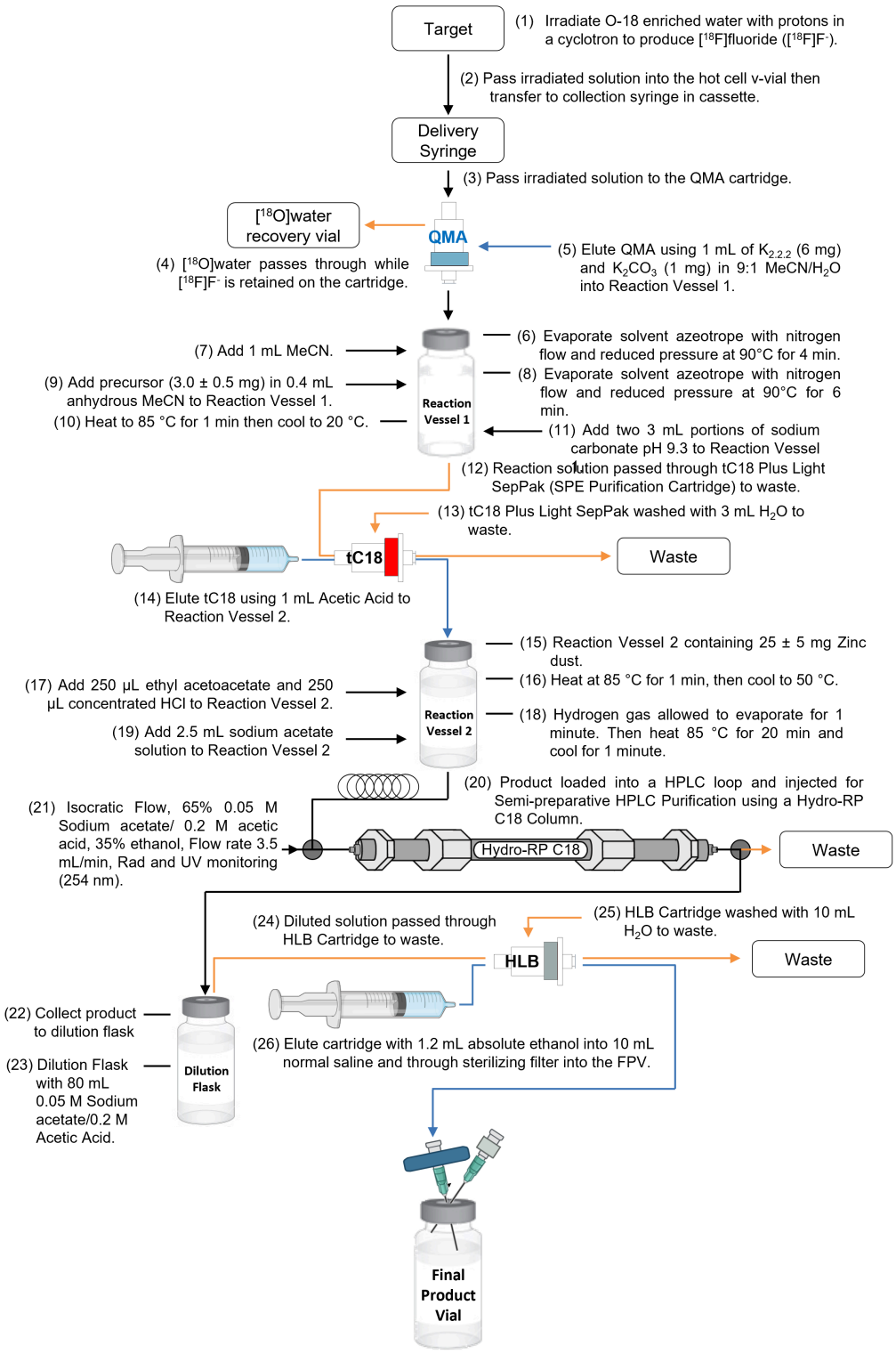


Figure 3

Schematic representation of the steps in the preparation of [^{18}F]Fluoroedaravone.

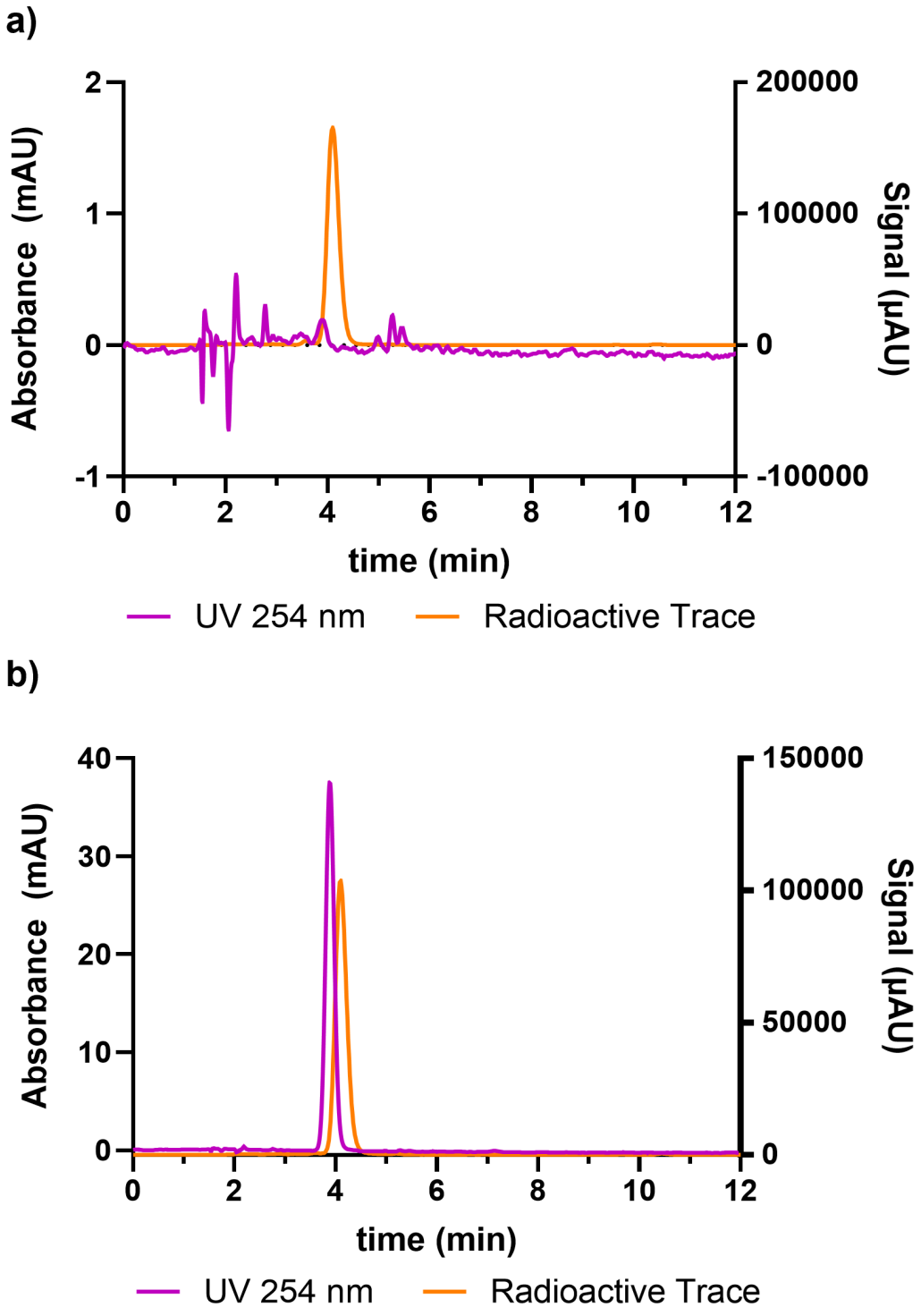


Figure 4

Analytical HPLC analysis of a) [^{18}F]Fluoroedaravone sample and b) 1:1 co-injection with the non-radioactive FEDV standard.

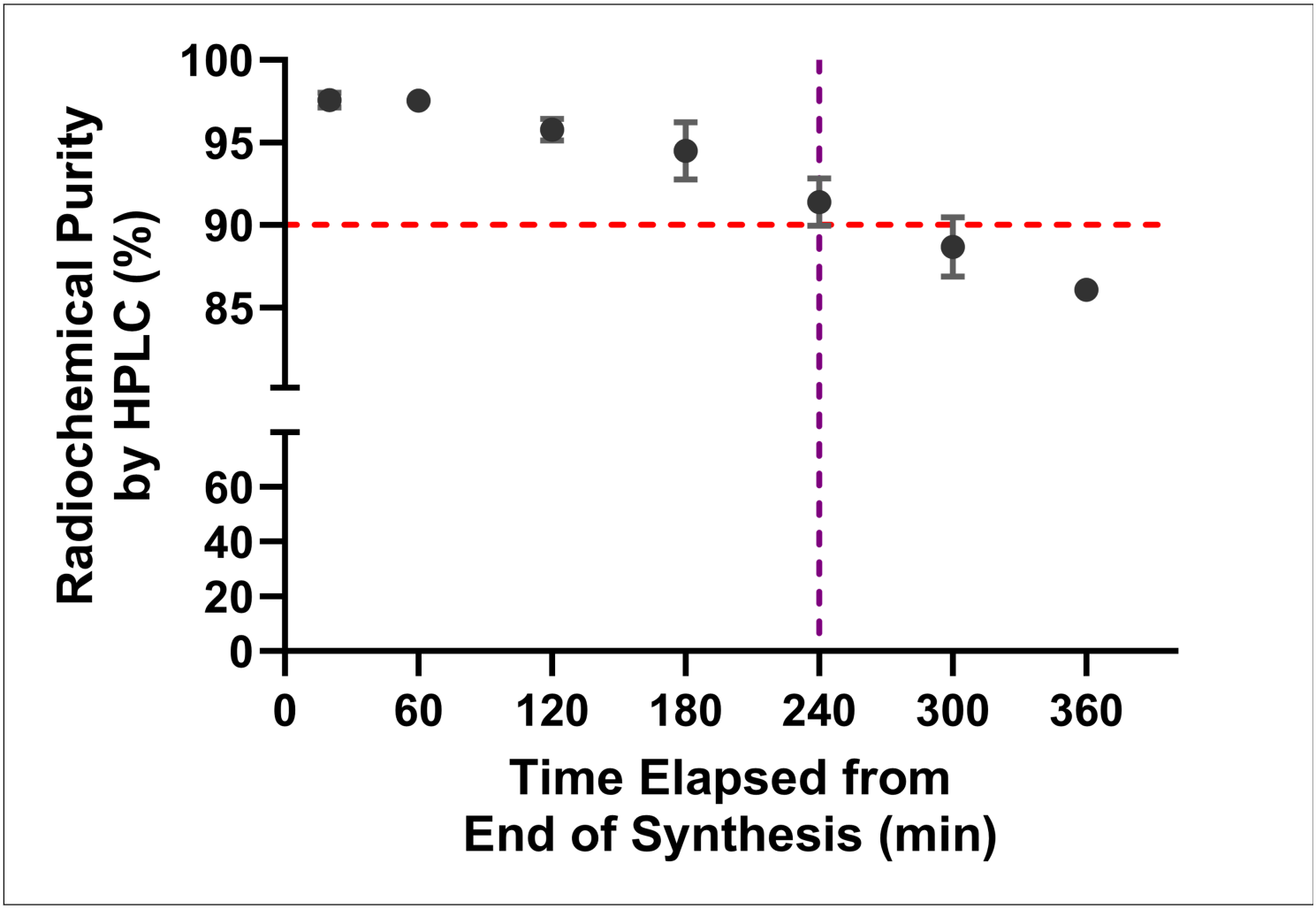


Figure 5

Stability analysis of [^{18}F]Fluoroedaravone (n = 3) in final dose formulation.

Supplementary Files

This is a list of supplementary files associated with this preprint. Click to download.

- FEDVTrasisAiosupplementalinfofinalGhoshetal..docx